Peculiarities of ionic transport in $Li_{1.3}Al_{0.15}Y_{0.15}Ti_{1.7}(PO_4)_3$ ceramics

2009 J. Phys.: Condens. Matter 21 185502

(http://iopscience.iop.org/0953-8984/21/18/185502)

J. Phys.: Condens. Matter **21** (2009) 185502 (7pp) doi:10.1088/0953-8984/21/18/185502

Peculiarities of ionic transport in $Li_{1.3}Al_{0.15}Y_{0.15}Ti_{1.7}(PO_4)_3$ ceramics

T Šalkus[1,5], E Kazakevičius[1], A Kežionis[1], A Dindune[2], Z Kanepe[2], J Ronis[2], J Emery[3], A Boulant[3], O Bohnke[4] and A F Orliukas[1]

[1] Department of Physics, Vilnius University, Sauletekio aleja 9/3, LT-10222, Vilnius, Lithuania
[2] Institute of Inorganic Chemistry, Riga Technical University, Miera iela 34, LV-2169 Salaspils, Latvia
[3] Laboratoire de Physique de l'Etat Condensé (UMR 6070 CNRS), Institut de Recherche en Ingénierie Moléculaire et Matériaux Fonctionnels (FR 2575 CNRS), Université du Maine, Avenue O Messiaen, 72085 Le Mans Cedex 9, France
[4] Laboratoire des Oxydes et Fluorures (UMR 6010 CNRS), Institut de Recherche en Ingénierie Moléculaire et Matériaux Fonctionnels (FR 2575 CNRS), Université du Maine, Avenue O Messiaen, 72085 Le Mans Cedex 9, France

E-mail: tomas.salkus@ff.vu.lt

Received 23 December 2008, in final form 2 March 2009
Published 31 March 2009
Online at stacks.iop.org/JPhysCM/21/185502

Abstract

A powder of $Li_{1.3}Al_{0.15}Y_{0.15}Ti_{1.7}(PO_4)_3$ has been synthesized by solid state reaction. The powder was a single phase material and had rhombohedral symmetry (space group $R\bar{3}c$) with six formula units in the unit cell. Impedance spectra of $Li_{1.3}Al_{0.15}Y_{0.15}Ti_{1.7}(PO_4)_3$ ceramics were recorded in the frequency range from 10^6 to 1.2×10^9 Hz and temperature range from 300 to 600 K. Two relaxation type dispersions of electrical quantities in the frequency range were found. The dispersion regions are presumably related to the ionic transport processes in bulk and grain boundaries of the ceramics. The activation energy of the conductivity of the bulk and the activation energy of the characteristic relaxation frequency, at which the dispersion sets in, has the same value of 0.25 eV. The only contribution of the mobility of Li^+ ions defines the temperature dependence of the bulk conductivity in the investigated temperature range. The values of ε' may be related to the contributions of the polarization of the fast ionic migration, vibrations of the lattice and electronic polarization. Nuclear magnetic resonance (NMR) investigation shows that the T_1 of ^{7}Li and ^{6}Li at room temperature are 6 ms and 2 s respectively. This result confirms that the relaxation of the ^{7}Li nucleus occurs through quadrupolar fluctuations although the relaxation of the ^{6}Li nucleus occurs via dipolar fluctuations. Furthermore, the T_1 minimum allows us to evidence a motion with a characteristic frequency in the range of the Larmor frequency.

1. Introduction

Solid electrolytes (SE) with fast Li^+ ion transport have emerged as attractive materials for applications in CO_2 gas sensors [1] and solid electrolyte batteries [2]. It has already been reported that the ionic conductivity (σ) of $LiTi_2(PO_4)_3$ increases appreciably if Ti^{4+} is partially substituted by Al^{3+}, Sc^{3+}, Fe^{3+}, Y^{3+}, Ga^{3+} ions (at room temperature the value of σ of $LiTi_2(PO_4)_3$ compound was found to be 7.9×10^{-6} S m^{-1}) [3–6]. The Li^+ ion transport number in these compounds was found to be $t_i = 1$ [7]. The total ionic conductivity of the system $Li_{1+x+y}Al_x(Y_y)Ti_{2-x-y}(PO_4)_3$ at $T = 298$ K has been found for the system $Li_{1+x}Al_xTi_{2-x}(PO_4)_3$ ($x = 0.3$) and for the system $Li_{1+y}Y_yTi_{2-y}(PO_4)_3$ ($y = 0.4$) to be 7×10^{-2} S m^{-1} and 6×10^{-2} S m^{-1}, respectively [7]. The substitution of Ti^{4+} by Al^{3+} with a smaller ionic radius causes the decrease of the unit cell dimensions of the NASICON framework, but enhances the conductivity for about three orders of

[5] Author to whom any correspondence should be addressed.

magnitude [8]. At room temperature $Li_{1+x}M_xTi_{2-x}(PO_4)_3$ (M = Al, Y, x = 0–0.7) belongs to the rhombohedral symmetry (space group $R\bar{3}c$) and is ascribed to the NASICON type compounds [9]. Li-conducting amorphous phase has been detected in $Li_{1+x}Al_xTi_{2-x}(PO_4)_3$ ($x > 0.5$) by ^{31}P and ^{27}Al magic angle spinning (MAS) NMR spectroscopy which accounts for the increase in the conductivity [9, 10]. In $Li_{1.3}Al_{0.3}Ti_{1.7}(PO_4)_3$ two relaxation dispersion processes were found related to ion transport in the bulk and grain boundaries of the ceramic samples [11]. The high ionic conductivity of these materials at low temperature and peculiarities of the ionic migration stimulate further investigations of the electrical and ionic transport properties in a wide frequency range. Investigation of the electric properties of materials with fast ion transport at high frequencies provides unique information on mass and charge transport, polarization phenomena and relaxation processes in such systems. The relaxation processes in SE manifest themselves in the frequency dispersion of four quantities: complex electrical conductivity ($\tilde{\sigma} = \sigma' + i\sigma''$), dielectric permittivity ($\tilde{\varepsilon} = \varepsilon' - i\varepsilon''$), impedance ($\tilde{Z} = Z' - iZ''$), where intrinsic electrical impedance $Z' = \rho' \frac{l}{S}$, $Z'' = \rho'' \frac{l}{S}$ (S is the electrode area, l is the sample length), and dielectric losses ($\tan\delta$), as well as in the temperature dependences of these quantities. The frequency dependence of the conductivity obeys the formula $\sigma(\omega) = \sigma_{dc} + A(T)\omega^{n(T)}$ and is valid for solid electrolyte materials [12].

The relaxation dispersion of the SE electrical quantities covers several decades on the frequency scale, and the values of the electrical quantities themselves may change by many decades. So, experimental techniques have to be able to measure these quantities over a wide range of frequencies. The majority of known methods [11–15] for the measurement of electrical parameters of SE materials are based on the measurement of the complex reflection coefficient of a coaxial waveguide loaded with the sample under investigation. However, it is difficult to measure precisely the amplitude of the reflected wave superimposed with the incident wave when their amplitudes differ by 1% or less. In the present paper the measurements of impedance spectra of the $Li_{1.3}Al_{0.15}Y_{0.15}Ti_{1.7}(PO_4)_3$ ceramics have been performed by the transmission microwave impedance spectrometer set-up [16]. The results of the investigation of ^7Li NMR spectra of $Li_{1.2}Ti_{1.8}Al_{0.2}(PO_4)_3$ have indicated local and long-range motions of lithium [11]. Furthermore, no information from NMR investigations is available on the double substituted compounds $Li_{1+x+y}Al_x(Y_y)Ti_{2-x-y}(PO_4)_3$.

In this paper we report technological synthesis conditions of the $Li_{1.3}Al_{0.15}Y_{0.15}Ti_{1.7}(PO_4)_3$ powder, sintering of the ceramic samples, the results of our investigations of x-ray diffraction (XRD), NMR and electrical properties of the compound in the frequency range from 10^6 to 1.2×10^9 Hz and temperature range from 300 to 600 K.

2. Experimental procedure

A powder of $Li_{1.3}Al_{0.15}Y_{0.15}Ti_{1.7}(PO_4)_3$ has been synthesized from a stoichiometric mixture of Li_2CO_3, Y_2O_3 (purity 99.999%), extra pure $NH_4H_2PO_4$, Al_2O_3 and TiO_2 by solid state reaction. The mixture was milled for 8 h in an agate mill in ethyl alcohol. After milling, the mixture was heated for 24 h at temperature T = 723 K. After heating, the mixture was placed in the ethyl alcohol and this liquid was milled for 12 h in the planetary mill again. After this process the powder was heated for 1 h at T = 1173 K and for 2 h at T = 1273 K. After each heating the powder was placed in the ethyl alcohol and milled in the planetary mill again. The fine powder was dried at T = 393 K for 24 h. The average grain sizes were found to be 1–5 μm. For investigation of NMR and electrical properties the ceramic samples were sintered. The powder was uniaxially cold-pressed at 300 MPa. The sintering of $Li_{1.3}Al_{0.15}Y_{0.15}Ti_{1.7}(PO_4)_3$ ceramic samples was conducted in air at T = 1403 K. The sintering duration of ceramics was 1 h. The measurements of electrical properties of $Li_{1.3}Al_{0.15}Y_{0.15}Ti_{1.7}(PO_4)_3$ ceramic samples were investigated in air by an impedance spectrometer set-up [16].

The structure parameters of $Li_{1.3}Al_{0.15}Y_{0.15}Ti_{1.7}(PO_4)_3$ were obtained at room temperature from the x-ray powder diffraction patterns using Cu Kα_1 radiation. The scanning rate of the 2Θ range from 6° to 80° was 1° min^{-1}.

^7Li NMR experiments were performed on an Avance DSX300 spectrometer (Bruker) working at Larmor frequencies, ν_0 = 116.642 MHz. MAS experiments were performed at room temperature while dynamic studies were carried out on static samples without spinning.

The ^7Li spectra and the relaxation times T_1 were measured as a function of temperature between 170 and 420 K. ^7Li NMR spectroscopy is a valuable tool to probe the mobile lithium ion properties in this material. ^7Li is a quadrupolar nucleus (I = 3/2) with a small quadrupolar momentum ($Q = -0.045 \times 10^{-28}$ m^2). In a low symmetry site, such a nucleus exhibits different transitions: a central transition (CT) between +1/2 and −1/2 levels, and external transitions ($\pm 1/2 \leftrightarrow \pm 3/2$).

The sample, glued on an altuglass substrate, was placed into a 5 mm coil. Between room temperature (RT) and 150 K the sample was cooled with a regulated nitrogen flow and between RT and 410 K it was heated with a regulated air flow. Temperature was regulated with a BVT 2000 controller. With this design it was possible to monitor the temperature at about ±0.1 K. The spin lattice relaxation time T_1 measurements have been performed by using a saturation recovery sequence. The radio frequency of the electrical field was 62.5 kHz with a t_{90} liquid pulse duration of 4 μs. This corresponds to a non-selective excitation. To improve the signal to noise ratio, either 64 or 128 transients were accumulated in the high and low temperature ranges respectively.

Owing to the I = 3/2 value of the ^7Li nucleus, two values of T_1 were expected with specific ratios in the slow regime (low temperature) and only one in the fast regime (high temperature) [17–21]. However, whatever the temperature, only one T_1 was necessary to account for the experimental magnetization. Therefore the following relationship was used to fit the data:

$$M_z(\tau) = M_0\left[1 - 2\alpha\exp(-\tau/T_1)\right] \quad (1)$$

where $M_z(\tau)$ is the magnetization and T_1 is the spin lattice relaxation time. T_1, M_0 and α are considered as free parameters

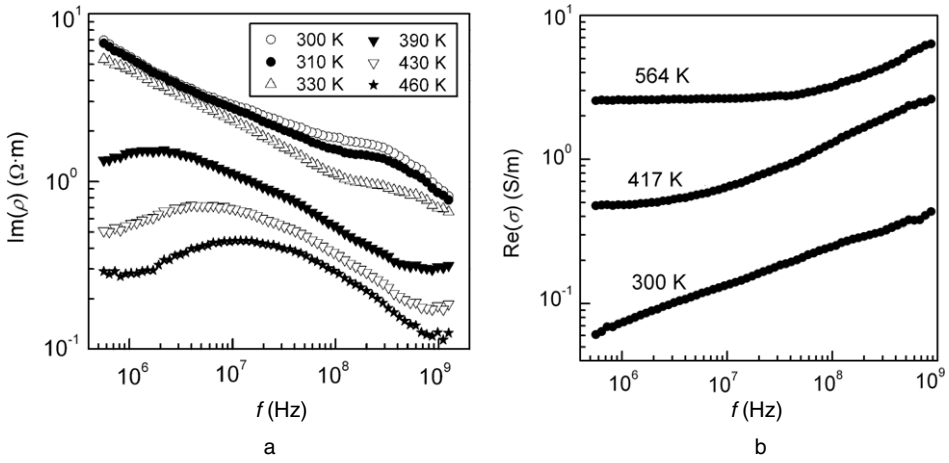

Figure 1. Frequency dependences of Im(ρ) (a) and Re(σ) (b) of $Li_{1.3}Al_{0.15}Y_{0.15}Ti_{1.7}(PO_4)_3$ ceramics at different temperatures.

in a least-squares fitting procedure. The T_1 values were determined by using either the peak area or the peak intensity of the magnetization recovery curve. The α parameter, which is not a critical one, is found to be around 0.5 for the saturation recovery method used in this work.

The DMFIT software is used to fit the spectra and obtain the peak linewidth, peak positions (in hertz or ppm), percentage and quadrupolar splitting [22]. ^{7}Li spectra are referenced from LiCl. Results are expressed either in hertz or in ppm (X(Hz) $= X$(ppm)ν_0(MHz)).

3. Results and discussion

The solid electrolyte $Li_{1.3}Al_{0.15}Y_{0.15}Ti_{1.7}(PO_4)_3$ compound was obtained by the substitution $Ti^{4+} \rightarrow [Al(Y)]^{3+} + Li^+$ in $LiTi_2(PO_4)_3$. The results of the x-ray investigation show the changes of the interplanar distances, (hkl) and relative intensity of the diffraction of crystals by incorporating Al and Y into $LiTi_2(PO_4)_3$.

The results of the x-ray diffraction study have shown that $Li_{1.3}Al_{0.15}Y_{0.15}Ti_{1.7}(PO_4)_3$ powder was a single phase material and belonged to the rhombohedral symmetry (space group $R\bar{3}c$) with six formula units in the unit cell. The lattice parameters, unit cell volume and theoretical density of the compound are presented in table 1.

The substitution of Ti^{4+} by Y^{3+} in $LiTi_2(PO_4)_3$ causes a decrease of the lattice parameters a, c, the volume V and increases the density of the compound. The density of the sintered $Li_{1.3}Al_{0.15}Y_{0.15}Ti_{1.7}(PO_4)_3$ ceramic sample was found to be 92% of the theoretically density.

Frequency dependences of the imaginary part of the complex impedance Im(ρ) and the real part of the complex electric conductivity Re(σ) at different temperatures are presented in figures 1(a) and (b), respectively.

Two dispersion regions were found in the Im(ρ) and Re(σ) spectra of $Li_{1.3}Al_{0.15}Y_{0.15}Ti_{1.7}(PO_4)_3$ ceramics. The dispersion processes are related to ion transport in the bulk and grain boundaries of the ceramics. Both processes are thermally activated and shift toward higher frequencies with increase of the temperature. The temperature dependence of the electrical

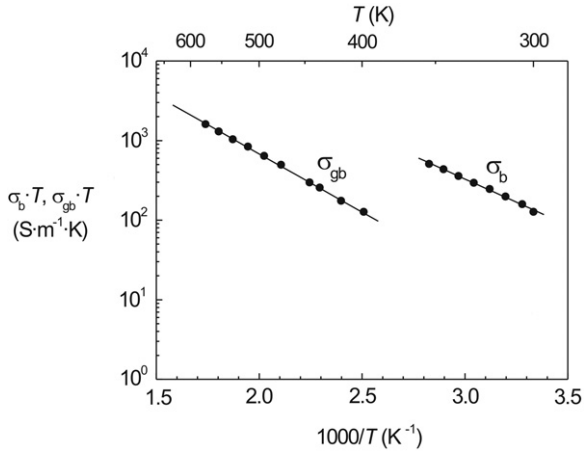

Figure 2. Temperature dependences of the bulk and grain boundary electrical conductivity of $Li_{1.3}Al_{0.15}Y_{0.15}Ti_{1.7}(PO_4)_3$ ceramics.

conductivity was derived from the $\rho''(\rho')$ and $\sigma''(\sigma')$ plots at different temperatures. Temperature dependences of the bulk (σ_b) and grain boundary (σ_{gb}) electric conductivity of $Li_{1.3}Al_{0.15}Y_{0.15}Ti_{1.7}(PO_4)_3$ ceramic samples are presented in figure 2.

At $T = 400$ K the value of σ_{gb} of $Li_{1.3}Al_{0.15}Y_{0.15}Ti_{1.7}(PO_4)_3$ was found to be 0.32 S m^{-1}. The σ_{gb} of the ceramic exponentially increases with increasing temperature in the entire temperature region. The activation energy of σ_{gb} of $Li_{1.3}Al_{0.15}Y_{0.15}Ti_{1.7}(PO_4)_3$ is $\Delta E_{gb} = 0.29$ eV. At 300 K the value of the bulk conductivity of $Li_{1.3}Al_{0.15}Y_{0.15}Ti_{1.7}(PO_4)_3$ was found to be 0.42 S m^{-1} and its activation energy $\Delta E_b = 0.25$ eV. The characteristic frequency f_b of the relaxation processes in the bulk at different temperatures is obtained from the maxima of the $\rho''(f)$ dependences.

In figure 3 the relaxation frequencies (f_b) of the dispersion of $Li_{1.3}Al_{0.15}Y_{0.15}Ti_{1.7}(PO_4)_3$ compound are shown as a function of the temperature.

At $T = 300$ K the value of f_b of $Li_{1.3}Al_{0.15}Y_{0.15}Ti_{1.7}(PO_4)_3$ was found to be 2.6×10^8 Hz. The relaxation frequency f_b increases with temperature according to the

Table 1. Lattice parameters and density of the $LiTi_2(PO_4)_3$ [23], $Li_{1.3}Al_{0.3}Ti_{1.7}(PO_4)_3$ [4], $Li_{1.3}Y_{0.3}Ti_{1.7}(PO_4)_3$ [5] and $Li_{1.3}Al_{0.15}Y_{0.15}Ti_{1.7}(PO_4)_3$ compounds.

Compound	Crystal symmetry	Lattice parameters (Å)	c/a	Unit cell volume V (Å^3)	Density d (g cm^{-3})
$LiTi_2(PO_4)_3$	Rhombohedral $R\bar{3}c$	$a = 8.5129(8)$ $c = 20.878(3)$	2.4525	1310.30	2.948
$Li_{1.3}Al_{0.3}Ti_{1.7}(PO_4)_3$	Rhombohedral $R\bar{3}c$	$a = 8.509(6)$ $c = 20.820(3)$	2.448	1304.3	2.928
$Li_{1.3}Y_{0.3}Ti_{1.7}(PO_4)_3$	Rhombohedral $R\bar{3}c$	$a = 8.5087(7)$ $c = 20.830(3)$	2.4481	1306.00	3.066
$Li_{1.3}Al_{0.15}Y_{0.15}Ti_{1.7}(PO_4)_3$	Rhombohedral $R\bar{3}c$	$a = 8.5069(6)$ $c = 20.8226(1)$	2.4477	1305.0	2.998

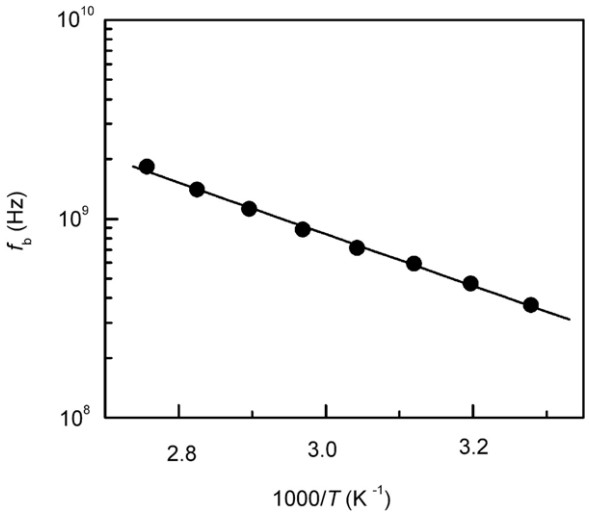

Figure 3. Temperature dependences of the relaxation frequency f_b of the bulk conductivity of $Li_{1.3}Al_{0.15}Y_{0.15}Ti_{1.7}(PO_4)_3$ ceramics.

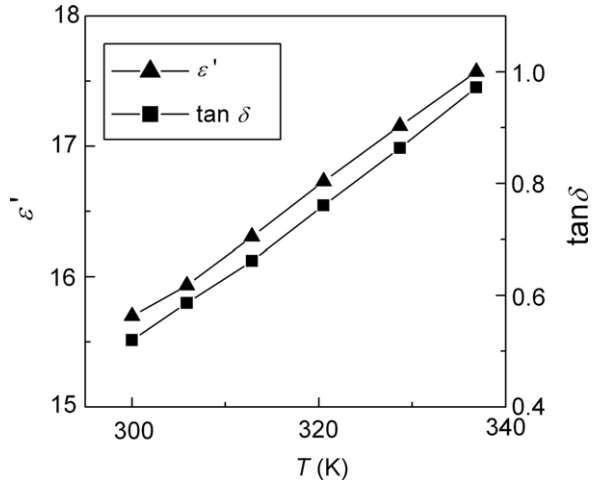

Figure 4. Temperature dependences of the permittivity and tan δ of $Li_{1.3}Al_{0.15}Y_{0.15}Ti_{1.7}(PO_4)_3$ compound at 1 GHz frequency.

Arrhenius law: $f_b = f_0 \exp(-\Delta E_f/kT)$, where f_0 is an attempt frequency, related to the phonon. The activation energy (ΔE_f) was calculated from the temperature dependence of the relaxation frequency in the bulk of the ceramic sample. The value of ΔE_f is 0.26 eV and is in good agreement with the value of ΔE_b. This fact leads to the conclusion that the temperature dependence of σ_b is a determinant of the temperature dependence of the mobility of the fast Li^+ ions. Such ion transport peculiarities are dominant in Li^+, Na^+ and oxygen vacancy solid electrolytes [4, 5, 24, 25].

The temperature dependences of the permittivity and tan δ were investigated at 1 GHz frequency. This frequency is higher than the Maxwell relaxation frequency $f_M = \sigma_b/2\pi\varepsilon_0\varepsilon'$ (where the dielectric constant of the vacuum $\varepsilon_0 = 8.85 \times 10^{-12}$ F m^{-1}). At the temperature 300 K for $Li_{1.3}Al_{0.15}Y_{0.15}Ti_{1.7}(PO_4)_3$ the Maxwell relaxation frequency was found to be $f_M = 5.5 \times 10^8$ Hz. In figure 4 the permittivity and tan δ of $Li_{1.3}Al_{0.15}Y_{0.15}Ti_{1.7}(PO_4)_3$ compound is shown as a function of the temperature.

At $T = 300$ K the value of the permittivity of $Li_{1.3}Al_{0.15}Y_{0.15}Ti_{1.7}(PO_4)_3$ was found to be $\varepsilon' = 15.6$ and increases with temperature. The values of the permittivity of $Li_{1.3}Al_{0.15}Y_{0.15}Ti_{1.7}(PO_4)_3$ may be related to the contribution of the polarization of the fast ionic migration, vibrations of the lattice and electronic polarization. The increase of tan δ with temperature can be caused by the increase of the conductivity of the sample.

Figure 5 shows the ^{7}Li spectra recorded at 250 K in the static mode (figure 5(a)) and at 295 K in the MAS mode with the spinning frequency $\nu_R = 10$ kHz (figure 5(b)). These are typical spectra for a quadrupolar nucleus with spin $I = 3/2$ showing the central transition and the satellite transitions. The specific powder line shape presented in figure 5(a) originates from the first order quadrupolar interaction contribution given by the Hamiltonian:

$$H_Q = \hbar\omega_Q \sum_{m=-2}^{+2} (-1)^m \overline{\overline{V}}^{(2)}_{-m} \overline{\overline{T}}^{(2)}_{m} \tag{2}$$

with

$$\frac{e^2 q Q}{2I(2I-1)\hbar} = \omega_Q = \frac{C_Q}{2} \tag{3}$$

where $\overline{\overline{X}}_m$ ($X = T$ or V) is the m component of the second order irreducible tensor $\overline{\overline{X}}$. $\overline{\overline{T}}$ stands for the spin part of the quadrupolar interaction while $eq\overline{\overline{V}}(\theta, \phi)$ (the anisotropic spatial part) accounts for the local electric field gradient at the ^{7}Li site (the angles θ and ϕ identify the direction of the static magnetic field $\vec{B}_0$ in the principal axis system of the electric field gradient tensor). The quadrupolar interaction is

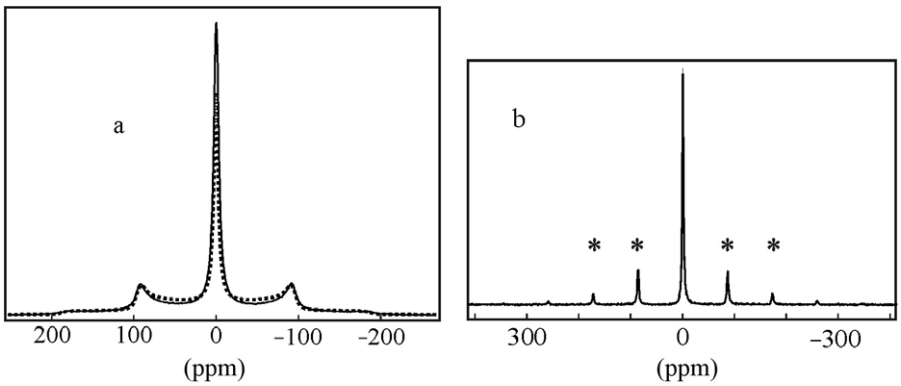

Figure 5. Single pulse acquisition. Experimental (full line) at 295 K and calculated (dotted line) ^{7}Li spectra acquired in the static mode: (a) the amplitude parameter was adjusted on the satellite amplitude, (b) MAS spectrum at the spinning frequency 10 kHz. Stars indicate the first spinning side bands. The fit parameters are $C_Q = 44$ kHz, $\eta_Q = 0$.

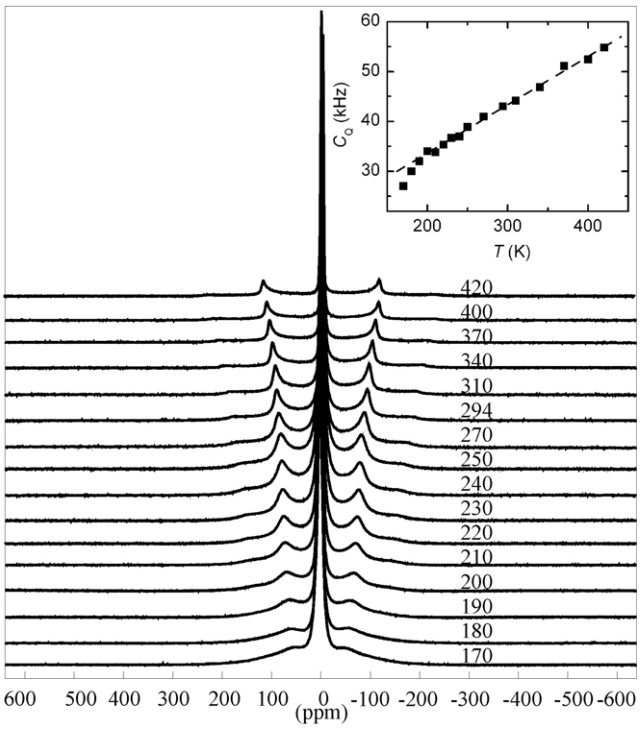

Figure 6. ^{7}Li spectra recorded at different temperatures in kelvin (inset: quadrupolar amplitude parameter versus temperature).

defined with its amplitude C_Q (kHz) or ω_Q and its asymmetry parameter η_Q.

The calculated spectra are also reported in figure 5(a) with the quadrupolar fitting parameters $C_Q = 44$ kHz and $\eta_Q = 0$. The results of the comparison [8, 9, 11] have shown that the linewidth of the central component of ^{7}Li MAS NMR spectra of the $Li_{1+x}Ti_{2-x}Al_x(PO_4)_3$ compounds is almost constant for $x \leqslant 0.2$ but increases for $x > 0.2$. The shift of this component from -1.20 to -0.7 ppm is observed. In samples with $x = 0.3$, 0.5 and 0.7 the ^{7}Li MAS NMR spectra are formed by two components with quadrupole constant $C_Q^{(1)} = 40$ kHz and $C_Q^{(2)} = 110$ kHz. The asymmetry parameter is $\eta = 0$ for different x [9]. The MAS spectrum in figure 5(b) is composed with the isotropic line (the most intensive one) flanked by several spinning side bands (less intensive marked with a star). The isotropic line does not evidence any second order quadrupolar effect and is fitted with only one Lorentzian line. So the ^{7}Li nuclei access to only one site in the structure. The spectrum is fitted with the same parameters as the ones used for the static spectrum. Generally two cavities are observed in these NASICON. Nevertheless, owing to the Li motion our spectrum can be fitted with a single quadrupolar contribution.

In figure 5(a) we observe that the amplitude of the central transition is more important than the satellite ones. This is a general feature in such systems because the quadrupolar interaction acts at the second order (of perturbation) on the central transition. So, in the presence of small disorder the satellite transitions are smoothed but it does not act on the central transition which appears more intensive. Among several other reasons, we can give two of them. The first one could be the dipolar interaction, the principal axes of which are different to that of the quadrupolar interaction and act more intensively on the satellite than on the central transition. The second one could be due to transverse relaxation where the adiabatic contribution disappears in the central transition [21]. In order to overcome this difficulty the quadrupolar echo sequence (not represented here) was performed, and gives correct relative intensities between the central line and the satellite ones. This confirms the presence of a single site contrarily to the results of Arbi *et al* [11].

In figure 6 we can observe that the splitting between the satellite transitions is sensitive to the temperature. This is due to the C_Q parameter variation, as reported in inset of figure 6. The satellite transitions appear more resolved when the temperature increases because the dipolar broadening is averaged by the motion. Below 200 K, the dipolar interaction smoothes the singularities associated to these transitions. So in the temperature range (170–420 K) in which the satellite transition become more resolved, the inverse of the fluctuation correlation time is between the amplitude of the dipolar interaction and the Larmor frequency ($\nu_0 = 116$ MHz). Nevertheless this better resolution can also arise through dynamical effects on the quadrupolar interaction: when the amplitude of the quadrupolar ω_Q interaction is in the range

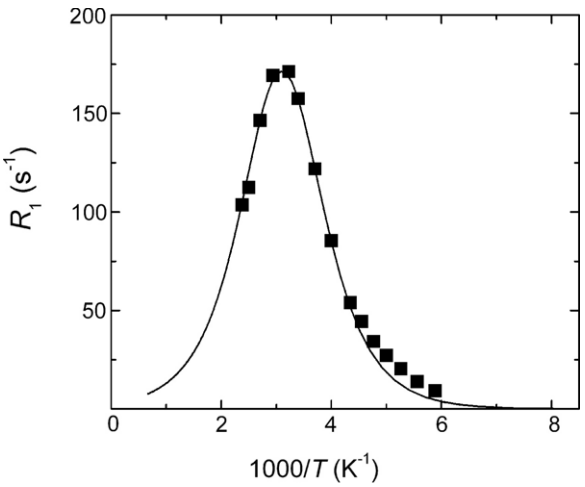

Figure 7. Experimental and calculated (continuous line) rate of the ^{7}Li spin lattice relaxation versus temperature.

of the inverse of the average correlation time of the motion $\omega_Q\tau_c \cong 1$ the motional process leads to a rapid decrease of the transverse magnetization.

Nevertheless, the behavior of the satellite transitions is a very surprising one: when the temperature increases the splitting between the satellite transitions increases. Generally it is expected that the splitting will be at least partially averaged by the motion when the temperature increases and the average value is weaker than the static one. However, it is worth noting that C_Q behaves in the same manner as in $LiTi_2(PO_4)_3$ [8]. This behavior indicates that the static (averaged) part of the electrical field gradient due to the environment of the ^{7}Li nucleus increases. Several scenarios could explain this behavior but the physical ones have to take the motion into account because the dipolar interaction and the linewidth are averaged. Whatever is the origin of this static component of the electrical field gradient (either the close neighbors of the Li^+ ions or longer distance contributions), it arises necessarily from the dynamical shift (see below) due to anisotropic motion. Only a better knowledge of the structure could help in the understanding of this dynamical mechanism.

Figure 7 shows the rate of the spin lattice relaxation R_1 ($R_1 = 1/T_1$) versus the reciprocal temperature obtained on the sintered material. Several features can be observed from this curve. First, it shows that the T_1 follows an activated law due to activated motion the correlation time of which is given by $\tau_c = \tau_{c0}\exp(\frac{E_a}{kT})$ with E_a the activation energy. Second, it exhibits a maximum around $T(R_1^{max}) = 325$ K. The T_1 of ^{7}Li at room temperature is 6 ms. Third, only one T_1 is observed whatever the regime. At the maximum of the R_1 curve the relation $\omega_0\tau_c \cong 1$ is verified, with $\tau_c \cong 1.3\times10^{-9}$ s the correlation time of the fluctuations which produce the relaxation and $\omega_0 = \gamma_{^7Li}B_0 = 2\pi\nu_0$. The parameter ν_0 is the ^{7}Li Larmor frequency (116 MHz) and $\gamma(^7Li)$ the gyromagnetic constant of the ^{7}Li nucleus. The minimum separates the fast regime ($\omega_0\tau_c \ll 1$ high temperature) and the slow regime ($\omega_0\tau_c \gg 1$).

The T_1 of ^{6}Li at room temperature is found to be around 2 s and the ratio is $\frac{T_{1(^7Li)}}{T_{1(^6Li)}} \approx 600$. This ratio is not 3600 but it is also far from the squared ratio between the γ gyromagnetic factors of the two nuclei involved in the hetero-nuclear spin–spin relaxation $[\frac{\gamma_{^7Li}}{\gamma_{^6Li}}]^2 \approx 7$. So we can conclude that the ^{6}Li nucleus relaxes with the dipolar fluctuations but the ^{7}Li nucleus mainly relaxes with the quadrupolar fluctuations.

It is now well established that, even in the presence of a single correlation time, in the slow regime two relaxation times T_1 characterize the magnetization equilibrium recovery [17–21] for an $I = 3/2$ spin system when only one relaxation time monitors the relaxation in the rapid regime. Unfortunately in solid samples the two relaxation times are difficult to observe, as in the present case [26–28]. So, in view of the experimental finding that the deviation from the exponential form is very small it is common to define a spin lattice relaxation rate as follows [28]:

$$\frac{1}{T_1} = \Omega_Q^2[J_1(\omega_0) + 4J_2(2\omega_0)] \tag{4}$$

with

$$\Omega_Q = \frac{1}{50}\left(1+\frac{\eta^2}{3}\right)^{1/2} e^2qQ/\hbar \tag{5}$$

and the spectral density $J_n(n\omega) = \frac{n^2\tau_c}{1+(n\omega\tau_c)^2}$ with $n = 1$ or 2 where τ_c is the correlation time.

According to this model, $1/T_1$ has been calculated and the result is shown as the full line in figure 7. Therefore we determined the parameter $\tau_{c0} = 6.2\times10^{-12}$ s, the activation energy $E_a = 0.14$ eV and $\Omega_Q = 540\times10^3$ rad s^{-1}. By using the relationship $\tau_c = \tau_{c0}\exp(\frac{E_a}{kT})$ the value of τ_c is found to be 0.9×10^{-9} s at the temperature of the R_1 maximum (325 K). This value is very close to the value of 0.85×10^{-9} s obtained by using the relationship $\omega_0\tau_c \cong 0.62$.

The fluctuation amplitude $[\Omega_Q(^7Li)]$ can be deduced from the R_1 maxima $[R_1(^7Li)]_{max} \approx \frac{[\Omega_Q(^7Li)]^2}{\omega_0(^7Li)}$ which provides $\Omega_Q(^7Li) = 360\times10^3$ rad s^{-1} which is in the range of the calculated value. This value is in the range of the quadrupolar parameter 295 K (figure 5) $C_Q = 276\times10^3$ rad s^{-1}.

This is an interesting result because the above relation of $1/T_1$ together with the spectral densities relationship are those used for reorientational motions with isotropic fluctuations, while the spectrum which evidences quadrupolar structure, even at high temperature, indicates that the motion is an anisotropic one. So the static behavior given by the spectrum seems to be inconsistent with the dynamical behavior and these results deserve further studies. Nevertheless we can imagine a process in which the fluctuations are isotropic but cannot average the quadrupolar splitting. Therefore, such a situation is consistent with the increase of the C_Q parameter with temperature.

4. Conclusions

A powder of $Li_{1.3}Al_{0.15}Y_{0.15}Ti_{1.7}(PO_4)_3$ compound has been synthesized by solid state reaction and studied by x-ray diffraction and high resolution NMR. The NMR investigations were performed on sintered ceramic samples. The investigation of the electrical properties of $Li_{1.3}Al_{0.15}Y_{0.15}Ti_{1.7}(PO_4)_3$ ceramics was carried out in the frequency range from 10^6 to

1.2×10^9 Hz and the temperature range 300–600 K by complex impedance spectroscopy. Two relaxation type dispersions of electrical parameters in the frequency range are found. The dispersion regions are presumably related to the ionic transport processes in grains and grain boundaries. The partial substitution of Al by Y in the system causes changes of the interplanar distances of the compounds, increase of the σ_b, σ_{gb} and decrease of the ΔE_b and ΔE_{gb}. At $T = 300$ K the values of bulk and grain boundary conductivities of $Li_{1.3}Al_{0.15}Y_{0.15}Ti_{1.7}(PO_4)_3$ ceramics were found to be $\sigma_b = 0.42$ S m^{-1} ($\Delta E_b = 0.25$ eV) and $\sigma_{gb} = 2.5 \times 10^{-2}$ S m^{-1} ($\Delta E_{gb} = 0.29$ eV) respectively. The results of our investigation showed that temperature dependence of σ_b is caused only by the mobility of the fast Li^+ ions, while the number of charge carriers remains constant with temperature. The values of ε' may be related to the contribution of the polarization of the fast ionic migration, vibrations of lattice and electronic polarization. NMR investigations revealed the presence of only one Li site in the lattice of the $Li_{1.3}Al_{0.15}Y_{0.15}Ti_{1.7}(PO_4)_3$ compound. The spin lattice relaxation time T_1 evidences one Li^+ motion ($E_a = 0.14$ eV with $\tau_{c0} = 6 \times 10^{-12}$ s). The T_1 of ^{7}Li and ^{6}Li at room temperature are 6 ms and 2 s respectively. This result confirms that the relaxation of the ^{7}Li nucleus occurs through the quadrupolar fluctuations although the relaxation of the ^{6}Li nucleus occurs via the dipolar ones. It will be important to probe some other frequency windows of the Li^+ ion dynamical properties, for example the spin lattice relaxation time in the rotating frame $T_{1\rho}$, which is sensitive to slow motion, could be compared to T_1 values obtained in this study. Such a strategy has already been applied in the study of the fast ion conductor $Li_{3x}La_{2/3-x}\square_{1/3-2x}TiO_3$ [27, 28] and allowed to evidence long and short distance motions. The ^{27}Al and ^{31}P NMR investigations would also be suitable in the study of the static and dynamical properties of the lithium ions' motion.

References

[1] Salam F and Weppner W 1999 *Ionics* **5** 355
[2] Broussely M, Planchot J P, Rigobert G, Vireu D and Sarre G 1997 *J. Power Sources* **68** 8
[3] Subramanian M A, Subramanian R and Clearfield A 1986 *Solid State Ion.* **18/19** 562
[4] Sobiestianskas R, Kežionis A, Kazakevičius E, Orliukas A, Dindune A, Kanepe Z and Ronis J 2000 *Lith. J. Phys.* **40** 183
[5] Sobiestianskas R, Dindune A, Kanepe Z, Ronis J, Kežionis A, Kazakevičius E and Orliukas A 2000 *Mater. Sci. Eng.* B **76** 184
[6] Lin Z-X, Yu H-J, Li S-C and Tian S-B 1986 *Solid State Ion.* **18/19** 549
[7] Atachi G, Imanka N, Aono H, Sugimoto E, Sadaoka Y, Yasuda N, Hara T and Nagata M 1991 *US Patent Specification* No. 4, 985, 317, Jan. 15
[8] Arbi K, Rojo J M and Sanz J 2007 *J. Eur. Ceram. Soc.* **27** 4215
[9] Arbi K, Mandal S, Rojo J M and Sanz J 2002 *Chem. Mater.* **14** 1091
[10] Aono H, Sugimoto E, Sodaoka Y, Imanaka N and Adachi G-Y 1990 *J. Electrochem. Soc.* **137** 1023
[11] Arbi K, Lazarraga M G, Ben Hassen Chehimi D, Ayadi-Trabelsi M, Rojo J M and Sanz J 2004 *Chem. Mater.* **16** 255
[12] Almond D P and West A R 1983 *Solid State Ion.* **9/10** 277
[13] Kežionis A, Orliukas A, Paulavičius K and Samulionis V 1991 *Mater. Sci. Forum* **76** 229
[14] Badot J C, Bianchi V, Baffier N and Belhadj-Tahar N 2002 *J. Phys.: Condens. Matter* **14** 6917
[15] Ragot F, Badot J C, Baffier N and Fourrier-Lamer A 1998 *Solid State Ion.* **106** 143
[16] Orliukas A F, Kežionis A and Kazakevičius E 2005 *Solid State Ion.* **176** 2037
[17] McLachlan A D 1964 *Proc. R. Soc.* A **280** 271
[18] Hubbard P S 1970 *J. Chem. Phys.* **53** 985
[19] Bull T E 1972 *J. Magn. Reson.* **8** 344
[20] Werbelow L G 1979 *J. Chem. Phys.* **70** 5381
[21] Petit D and Korb J P 1988 *Phys. Rev.* B **37** 5761
[22] Massiot D, Fayon F, Capron M, King I, Le Calvé S, Alonso B, Durand J O, Bujoli B, Gan Z and Hoaston G 2002 *Magn. Reson. Chem.* **40** 70
[23] ASTM 1992 X-ray powder diffraction file inorganic No. 35-754. Philadelphia, USA
[24] Bogusz W, Dygas J R, Krok F, Kežionis A, Sobiestianskas R, Kazakevičius E and Orliukas A 2001 *Phys. Status Solidi* a **183** 323
[25] Orliukas A, Bohac P, Sasaki K and Gauckler L J 1994 *Solid State Ion.* **72** 35
[26] Bloembergen N, Purcell E M and Pound R V 1948 *Phys. Rev.* **73** 679
[27] Emery J, Bohnke O, Fourquet J L, Buzare J Y, Florian P and Massiot D 2001 *C. R. Acad. Sci. Chim.* **4** 845
[28] Emery J, Bohnke O, Fourquet J L, Buzare J Y, Florian P and Massiot D 2002 *J. Phys.: Condens. Matter* **14** 523